The role of paraspinal muscle degeneration in coronal imbalance in patients with degenerative scoliosis

Abdukahar Kiram[1], Zongshan Hu[1], Gene Chi-Wai Man[2], Hongru Ma[1], Jie Li[1], Yanjie Xu[1], Zhikai Qian[3], Zezhang Zhu[1,3], Zhen Liu[1,3], Yong Qiu[1,3]

[1]Division of Spine Surgery, Department of Orthopedic Surgery, Nanjing Drum Tower Hospital, The Affiliated Hospital of Nanjing University Medical School, Nanjing, China; [2]Department of Orthopedics and Traumatology, The Faculty of Medicine, Prince of Wales Hospital, The Chinese University of Hong Kong, Hong Kong, China; [3]Department of Spine Surgery, Nanjing Drum Tower Hospital, the Clinical College of Nanjing Medical University, Nanjing, China

Contributions: (I) Conception and design: Z Liu; (II) Administrative support: Y Qiu; (III) Provision of study materials or patients: A Kiram, H Ma, Y Xu, Z Qian; (IV) Collection and assembly of data: Z Hu, A Kiram; (V) Data analysis and interpretation: A Kiram, Z Hu, GCW Man, Z Liu, Z Zhu, Y Qiu; (VI) Manuscript writing: All authors; (VII) Final approval of manuscript: All authors.

Correspondence to: Yong Qiu. Professor, Spine Surgery, Affiliated Drum Tower Hospital of Nanjing, University Medical School, Zhongshan Road 321, Nanjing 210008, China. Email: scoliosis2002@sina.com.

Background: Coronal imbalance in degenerative scoliosis is common and is highly correlated with health-related quality of life. Paraspinal muscle is critical to spine stability, but little is known about its contribution to coronal imbalance in degenerative scoliosis. This study aims to investigate the relationship between paraspinal muscle (PSM) degeneration and coronal imbalance in patients with degenerative scoliosis (DS).

Methods: This is a retrospective cohort study. A total of 117 patients with DS were retrospectively reviewed. Parameters of PSM (bilateral cross-sectional area, CSA; fat infiltration rate, FI%) at the apical disc and adjacent levels were quantitatively evaluated using MRI. Standing whole-spine radiograph was used to evaluate the coronal (Cobb angle, CA; coronal balance distance, CBD) and sagittal (thoracic kyphosis, TK; lumbar lordosis, LL; sagittal vertical axis, SVA) parameters. Patients were divided into 3 groups: coronal balanced (Type A), coronal imbalanced shifting to concavity (Type B), and coronal imbalanced shifting to convexity (Type C).

Results: Based on our criteria, 56 patients were assigned to Type A, 34 patients to Type B, and 27 patients to Type C. There was no significant difference on the sagittal profiles and CSA between the groups. However, Type A showed significantly lower FI% than Type B and Type C on both concavity and convexity (Concave side: Type A *vs.* Type B *vs.* Type C, 30.8±8.1 *vs.* 45.1±7.7 *vs.* 38.7±12.5, P=0.001; Convex side: Type A *vs.* Type B *vs.* Type C, 32.6±10.9 *vs.* 46.3±7.3 *vs.* 40.7±11.8, P=0.004). Specifically, Cobb angle was negatively correlated with CSA, mainly at convexity (R=−0.415, P=0.008). Similarly, the increase of CBD significantly correlated with FI% at concavity (R=0.491, P=0.001) and convexity (R=0.354, P=0.025).

Conclusions: DS patients with coronal imbalance demonstrated a worse PSM degeneration when compared with those without coronal imbalance. Besides, PSM degeneration strongly correlated with coronal imbalance, which implies that PSM degeneration may contribute to the coronal imbalance in patients with DS.

Keywords: Degenerative scoliosis (DS); paraspinal muscle (PSM); fat infiltration rate; coronal imbalance; adult spinal deformity

---

5102

Kiram et al. Paraspinal muscle degeneration in coronal imbalance

Introduction

Degenerative scoliosis (DS) is a three-dimensional spinal deformity, often accompanies with sagittal and coronal malalignment, that usually occurs in female patients over 50 years of age (1,2). This is generally associated with back pain, lower-limb pain, and functional impairment (3). With an aging population worldwide, DS is a considerable healthcare concern which accounts for 13.3% of the Chinese population aged 40 and above. Although the exact pathogenesis of DS remains unknown, the progression and asymmetric degenerative changes involving the vertebrae, intervertebral discs and facet joints are major factors for the spinal column malalignment (4).

The paraspinal muscle (PSM) are comprised of the psoas, quadratus lumborum, multifidus (MF), and erector spinae (ES) (5,6). In recent years, the involvement of PSM toward the occurrence and development of spinal deformity have been heavily debated (7). Several studies had reported that poor PSM quality was associated with the occurrence of lower back pain, spinal stenosis, and disc herniation, as well as spinal deformity (7-10). Yet, as most of these studies only focused on their relationship with sagittal parameters, it neglects their correlation with coronal imbalance. Unlike the rare occurrence in adolescent idiopathic scoliosis (AIS), coronal imbalance plays a pivotal role toward the progression and development of DS (7,11).

As one of the most common manifestations in DS, the prevalence of coronal imbalance occurred in 34.8% of Chinese patients (12). In addition, coronal imbalance in patients with DS is highly correlated with decreased health-related quality of life (HRQoL) (13). Whatsmore, the occurrence of coronal imbalance increases the likelihood of implant-related failure, which may require revision surgery (14). In clinical practice, we observe DS patients displays various coronal imbalance even Cobb angle of main curve remains similar. Accordingly, our research team developed a new classification system, namely Nanjing classification, based on preoperative coronal balance distance (CBD) and inclination pattern. Importantly, this system has provided new insights regarding surgical decision-making, especially for patients with type C who prone to coronal imbalance after 3-column osteotomy (15-18). Although, lumbosacral fractional curve, L4 tilt and apex location were shown to be related to coronal imbalance, there remains a scarce of literature comprehensively describing etiology of different

pattern of coronal imbalance (18). Hence, we speculated that paraspinal muscle degeneration may variate among the different subtypes based on our Nanjing classification. Based on study from Sun *et al.* (11), they found CBD was correlated with lumbar multifidus atrophy in DS patients. Xie *at al.* (19) reported positive correlation between Cobb angles with asymmetric degree of multifidus muscle. However, to the best of our knowledge, there are scarce of literatures investigating the relationship between PSM degeneration and coronal imbalance in DS patients. Hence, in this study, we aimed to compare the morphological differences of PSM degeneration between DS patients with and without coronal imbalance, and to investigate the relationship between PSM degeneration and coronal imbalance in DS patients. We present the following article in accordance with the STROBE reporting checklist (available at https://qims.amegroups. com/article/view/10.21037/qims-22-222/rc).

Methods

Patient selection

The quality and quantity of paraspinal muscle were reported to be correlated with age and gender (20,21). To eliminate those confounding factors, this retrospective cohort study included female patients with DS that attended our hospital during the period from February 2017 to December 2020. Inclusion criteria were those aged between 50 to 75 years old at the time of attendance, medical records containing anteroposterior and lateral X-ray radiographs of total spine and magnetic resonance imaging (MRI) of the lumbar spine, and Cobb angle of lumbar curve in the coronal plane >20° on a standing posteroanterior film. Exclusion criteria were history of scoliosis in childhood or adolescence, history of spinal surgery, local infection, inflammation around the spine, history of severe spinal trauma, spinal tumor, and presence of other systemic diseases that can affect spinal alignment (e.g., muscular dystrophy, ankylosing spondylitis, Parkinson disease, etc.) (*Figure 1*). In addition, basic demographic data, including age, weight, and height, were also obtained. The study was conducted in accordance with the Declaration of Helsinki (as revised in 2013). The study was approved by institutional review board (No. 2021-LCYJ-DBZ-05). All volunteers were fully informed about the methods, purposes, and risks involved in the study protocol and signed the informed consent.
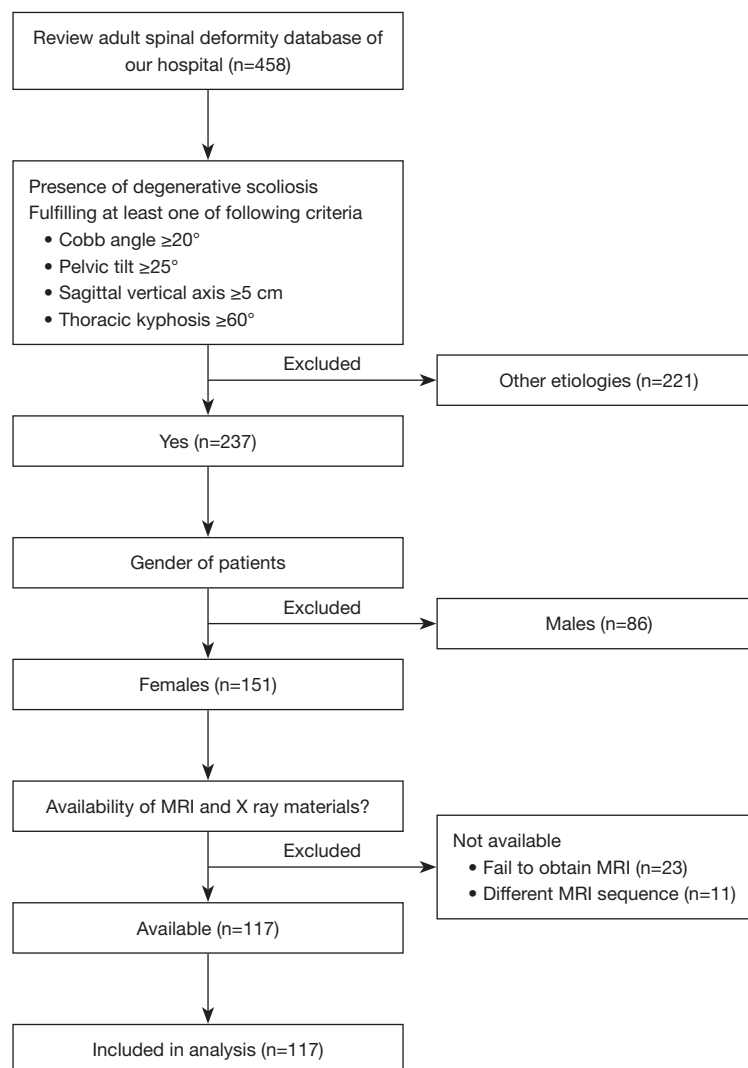
Figure 1 Workflow of this study.

Radiological assessment

A full-spine anteroposterior and lateral radiograph was obtained for patients enrolled in this study. Radiographic parameters were measured on X-ray films according to the Spine Deformity Study Group guidelines, including coronal and sagittal parameters (22). Coronal parameters include Cobb angle of main curve, location of apex vertebrae and coronal balance distance (CBD). The CBD is defined as the horizontal distance between C7 plum line and central sacral vertical line (CSVL). While for sagittal parameters, the measurements include sagittal vertical axis (SVA), thoracic kyphosis (TK) and lumbar lordosis (LL). The SVA is defined as the horizontal distance between

the vertical-line from the midpoint of C7 vertebrae to the posterior upper endplate of sacrum. The measurement of TK and LL refers the Cobb angle between T5 and T12 and the Cobb angle between L1 and S1, respectively. All measurements were attained by Surgimap (v2.3.2.1, Nemaris Inc, New York, NY).

Patients classification

After enrollment, patients were classified into three subtypes (Type A, B and C) according to Nanjing classification (15). The C7 plumb line (C7PL) is defined as the vertical line across the midpoint of C7 vertebrae. Based on the CBD and C7PL, the three subtypes of coronal imbalance were then
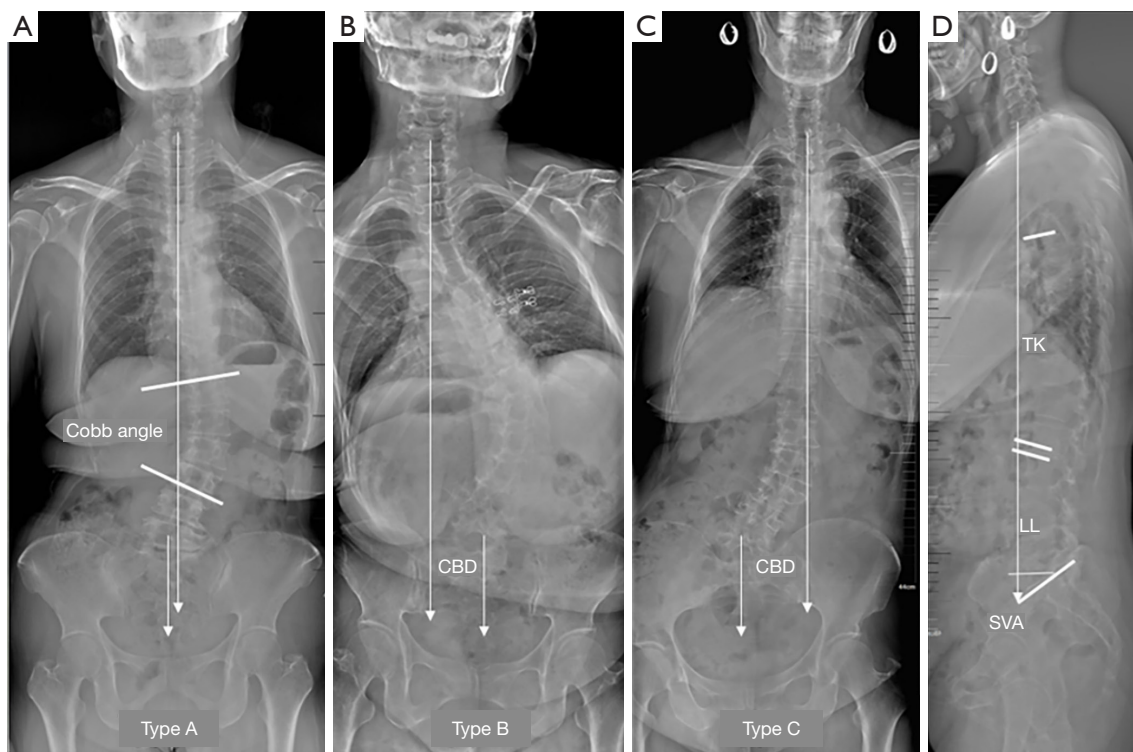
Figure 2 Three-part classification for coronal alignment based on severity and directionality relative to the thoracolumbar curve's concavity and convexity, based on Bao *et al.* (15). (A) Type A alignment has no coronal imbalance (trunk shift <3 cm); (B) type B with coronal imbalance (trunk shift >3 cm) and C7PL shifted to concave; (C) type C with coronal imbalance (trunk shift >3 cm) and C7PL shifted to convex side; (D) image of the measurement of TK and SVA performed on sagittal position. TK, thoracic kyphosis; SVA, sagittal vertical axis; CBD, coronal balance distance.

determined (*Figure 2*):

- ❖ Type A: patients with no coronal imbalance (trunk shift <3 cm),
- ❖ Type B: patients with coronal imbalance (trunk shift >3 cm) and a C7PL shifted to concave side, and
- ❖ Type C: patients with coronal imbalance (trunk shift >3 cm) and a C7PL shifted to convex side.

Magnetic resonance imaging (MRI)

The routine lumbar MRI images was acquired on the routine 1.5-T sigma imaging system (Magetom Skyra, Siemens healthcare, Erlagen, Germany). After scanning, the trans-axial and sagittal sequence of T2 weighted images were saved with DICOM format from picture archiving and communicating system (PACS). The sagittal sequence was used to identify the lower endplate of lumbar vertebrae. A total of 5 trans-axial slices, which located at apex level and 2 proximal and 2 distal levels, were obtained with 4 mm thickness and 2 mm space, shown in *Figure 3*.

Bilateral cross-sectional area (CSAs) of PSM was quantified by outlining the thoracolumbar facial boundary at targeted trans-axial slices using *ImageJ* image analyzing software (Image J ver. 1.3; NIH, Bethesda, MA). Fat infiltration rate (FI%) of PSM was obtained by pseudo-coloring technique as previously reported (19,23). Bilateral average CSAs and FI% of PSM was calculated and referred as total CSA and total FI% of lumbar PSM (*Figure 4*).

Method reliability

To evaluate the reliability of the measurements on the radiographs and MRI, the parameters were measured by two independent observers (HK and ZS). All these observers were blinded to the subject information. Intra-observer and inter-observer variations were estimated by using intraclass correlation coefficient (ICC), which were graded using previously described semi-quantitative criteria: excellent (ICC ≤0.9), good (0.7≤ ICC <0.9), acceptable (0.6≤ ICC <0.7), poor (0.5≤ ICC <0.6), or unpredictable (ICC <0.5) (22,24).
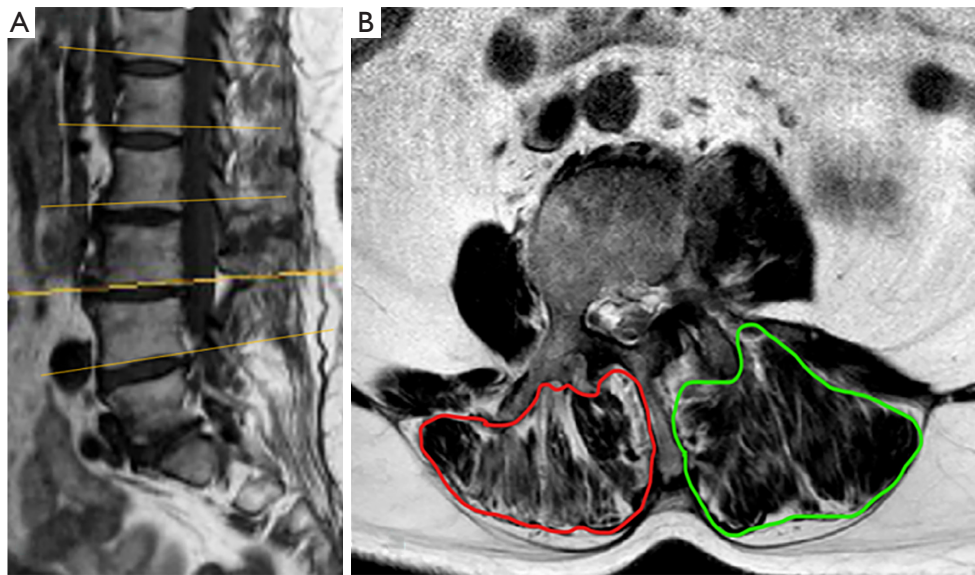
Figure 3 Sagittal (A) and trans-axial (B) MRI image. Yellow lines show the levels evaluated in this study and the area circled by red line shows paraspinal muscle in convex side and green line demonstrates the paraspinal muscle in concave side of the curve. MRI, magnetic resonance imaging.

Statistical analysis

The data is presented as means ± standard deviation. Data analysis was carried out using SPSS software (Version 23.0; SPSS, Chicago, IL, USA). Data was tested for normality by Kolmogorov-Smirnov test which presented a normal distribution. Demographics and radiographic parameters were compared between the three groups. One-way ANOVA and Bonferroni Post-hoc test was used for inter-group comparisons. Pearson's correlation test was used to analyze the correlation between different parameters. P value <0.05 was considered statistically significant.

The primary aim of the study is to investigate the relationship between PSM degeneration and with and without coronal imbalance in DS patients. Hence, cross-sectional area of PSM will be the primary comparison. Based on our pilot analysis, the comparison of DS patients with and without coronal imbalance showed an effective size of 0.48. Therefore, sample sizes of at least 50 patients without coronal imbalance (Type A) and 50 with coronal imbalance (Type B and C) will be needed to achieve an 81% power to detect the difference between the groups, with a significance level (alpha) of 0.05 (PASS 11.0, NCSS, LLC, Utah, USA).

Results

Demographic data

A total of 117 patients (117 females; average age 60.9± 5.2 years) were included in this study for analysis. The majority of patients had type A coronal alignment (CSVL <3 cm; Type A =56). Coronal malalignment consisting of type B (trunk shift ipsilateral to curve's concavity >3 cm; Type B =34) and type C (trunk shift ipsilateral to curve's convexity >3 cm; Type C =27) were less common. Their demography is shown in *Table 1*. There were no significant differences in the demographic data, which were screened by two experienced orthopedic surgeons (HK and ZS).

Comparison on radiographic data

The intra- and interobserver ICCs for estimating the sagittal parameters were from 0.83 to 0.96, suggesting good to excellent reliability of these measurements among the two observers (*Table 2*). There was no statistically significant difference for sagittal parameters, including SVA (Type A *vs.* Type B: 4.5±3.4 *vs.* 8.0±5.4, P=0.073; Type A *vs.* Type C: 4.5±3.4 *vs.* 7.3±6.8, P=0.147; Type B *vs.* Type C: 8.0±5.4 *vs.* 7.3±6.8, P=0.756; Type A *vs.* Type B *vs.* Type C: 4.5±3.4 *vs.* 8.0±5.4 *vs.* 7.3±6.8, P=0.134), TK (Type A

5106

Kiram et al. Paraspinal muscle degeneration in coronal imbalance
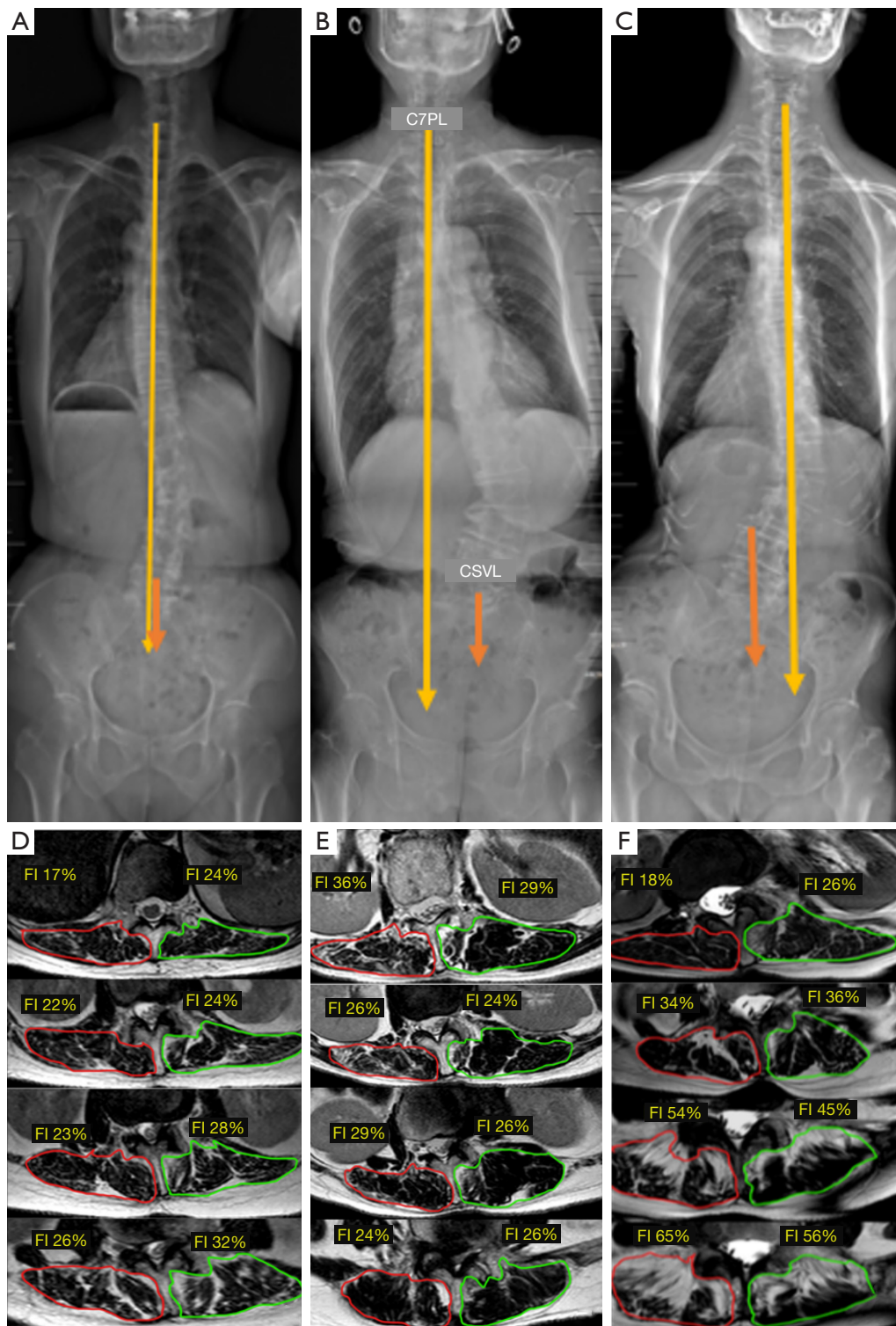

Figure 4 Comparison of paraspinal muscle between the different group of patients. (A-C) Radiographical plain of Type A, B and C. (D,E) The quantity and quality of paraspinal muscle at apex-2, apex-1, apex and apex+1 level in patient with type A and B. (F) The quantity and quality of paraspinal muscle at apex-1, apex and apex+1 and apex+2 level in patient with Type C. The margin of paraspinal muscle at concave and concave side were circled by red and green. C7PL, C7 plumb line, yellow axis; CSVL, central sacral vertical line, brown axis.

Table 1 Patient demographics

Demographics	All	Type A	Type B	Type C	P value
N	117	56	34	27	N/A
Gender	Female	Female	Female	Female	N/A
Age (years)	60.9±5.2	61.0±5.4	61.8±4.9	59.9±5.5	0.726
Height (cm)	156.6±7.3	158.0±7.3	154.2±8.1	156.4±6.6	0.428
Weight (kg)	58.6±6.9	60.4±7.3	57.5±7.4	56.0±4.7	0.222
BMI (kg/m^2)	23.8±1.6	24.1±1.3	24.1±1.8	22.9±1.9	0.128

Data are expressed as mean ± standard deviation. BMI, body mass index; N/A, not available.

Table 2 Intra- and inter-rater reliability test for all radiographic and MRI parameters

Parameters	Intra-rater coefficient	Inter-rater coefficient
Radiographic parameters		
Cobb angle (°)	0.91	0.95
CBD (cm)	0.91	0.83
SVA (cm)	0.93	0.90
TK (°)	0.95	0.92
LL (°)	0.96	0.95
MRI parameters		
CSA (cm^2)	0.90	0.83
FI%	0.96	0.91

CBD, coronal balance distance; CSA, cross sectional area; FI%, fat infiltration; LL, lumbar lordosis; MRI, magnetic resonance imaging; SVA, sagittal vertical axis; TK, thoracic kyphosis.

vs. Type B: 20.7±13.1 *vs.* 18.3±11.2, P=0.599; Type A *vs.* Type C: 20.7±13.1 *vs.* 12.9±8.0, P= 0.090; Type B *vs.* Type C: 18.3±11.2 *vs.* 12.9±8.0, P=0.300; Type A *vs.* Type B *vs.* Type C: 20.7±13.1 *vs.* 18.3±11.2 *vs.* 12.9±8.0, P=0.232) and LL (Type A *vs.* Type B: 22.3±15.0 *vs.* 28.0±16.3, P=0.367; Type A *vs.* Type C: 22.3±15.0 *vs.* 27.1±18.1, P=0.895; Type B *vs.* Type C: 28.0±16.3 *vs.* 27.1±18.1, P=0.895; Type A *vs.* Type B *vs.* Type C: 22.3±15.0 *vs.* 28.0±16.3 *vs.* 27.1±18.1, P=0.591) as shown in *Table 3*.

There were no statistically differences in terms of curve magnitude between Type A and Type B (36.6±11.1 *vs.* 40.7±7.9, P=0.313), Type A and Type C (36.6±11.1 *vs.* 33.8±10.8, P=0.489) and Type B and Type C (40.7±7.9 *vs.* 33.8±10.8, P=0.145). On the other hand, CBD is higher in both Type B and Type C while compared to CBD in Type A (Type A *vs.* Type B: 1.1±0.8 *vs.* 5.0±1.1, P<0.01; Type

A *vs.* Type C: 1.1±0.8 *vs.* 4.2±1.4, P<0.01). There was no significant difference in CBD between Type B and Type C (Type B *vs.* Type C: 1.1±0.8 *vs.* 4.2±1.4, P=0.084).

Comparison of CSA and FI% between three subtypes of coronal imbalance

The CSA and FI% of PSM from Apex-2 to Apex+2 level is shown in *Table 4*. No significant difference in terms of CSA between the three Types on both convex and concave sides (P>0.05). Whereas for the FI% of PSM, patients in Type B and Type C showed higher FI% than those in Type A in both concave and convex side. The intra- and interobserver ICCs for estimating the MRI parameters were from 0.83 to 0.96, suggesting good to excellent reliability of these measurements among the two observers (*Table 2*).

Correlation of CSAs and FI% of PSM with coronal parameters

In the correlation analysis, Cobb angle was negatively correlated with the CSA at apex vertebra translation in concave (R=−0.431, P=0.006) and convex side (R=−0.440, P=0.004) (*Table 5*). When assessing the total CSA, there was significant negative correlation between Cobb angle and the total CSA of paraspinal muscle (PSM) in convex side (R=−0.415, P=0.008). However, there no significant correlation between coronal balance distance (CBD), sagittal vertical axis (SVA), thoracic kyphosis (TK) and lumbar lordosis (LL) with the CSA at apex vertebra translation in concave and convex side (*Table 5*).

Toward the correlation on FI%, CBD was positively correlated with the CSA at apex vertebra translation in the concave side (R=0.349, P=0.027) (*Table 6*). When assessing the total FI%, there was significant positive correlation

Table 3 Radiographic parameters

Parameters	Type A (n=56)	Type B (n=34)	Type C (n=27)	P value			
				A *vs.* B *vs.* C	A *vs.* B	A *vs.* C	B *vs.* C
Coronal parameters							
Cobb angle (°)	36.6±11.1	40.7±7.9	33.8±10.8	0.334	0.313	0.489	0.145
Curve apex	2.1±0.6	2.2±0.6	2.0±0.5	0.760	0.670	0.670	0.462
CBD (cm)	1.1±0.8	5.0±1.1	4.2±1.4	<0.001	<0.001	<0.001	0.084
Sagittal parameters							
SVA (cm)	4.5±3.4	8.0±5.4	7.3±6.8	0.134	0.073	0.147	0.756
TK (°)	20.7±13.1	18.3±11.2	12.9±8.0	0.232	0.599	0.090	0.300
LL (°)	22.3±15.0	28.0±16.3	27.1±18.1	0.591	0.367	0.452	0.895

Data are expressed as mean ± standard deviation. CBD, coronal balance distance; SVA, sagittal vertical axis; TK, thoracic kyphosis; LL, lumbar lordosis.

Table 4 Comparison on concave or convex cross-sectional area and fat infiltration at the upper or lower intervertebral level of the apical vertebra

Variables	Concavity				Convexity			
	Type A (n=56)	Type B (n=34)	Type C (n=27)	P value	Type A (n=56)	Type B (n=34)	Type C (n=27)	P value
Cross-sectional area of PSM (cm^2)								
Apex-2	16.9±3.6	17.4±2.4	16.9±4.0	0.911	15.8±3.3	13.6±5.7	15.7±3.6	0.351
Apex-1	18.6±3.7	19.4±2.4	20.1±3.3	0.483	17.8±4.1	15.6±8.0	17.3±3.4	0.542
Apex	19.2±4.1	19.7±3.2	21.2±4.9	0.473	17.9±5.1	15.3±8.1	16.1±5.1	0.504
Apex+1	18.3±4.4	17.1±4.3	18.7±6.3	0.754	18.3±4.8	16.0±6.7	17.1±5.2	0.545
Apex+2	16.2±4.0	16.4±4.0	17.3±5.7	0.819	17.3±3.9	16.1±5.3	18.2±5.5	0.609
Total	17.8±3.3	18.0±2.5	18.9±3.6	0.718	17.4±3.5	15.3±6.4	16.9±3.3	0.467
Fat infiltration rate of PSM (%)								
Apex-2	24.7±9.2	42.8±2.4[a]	31.7±11.7[b,c]	<0.001	27.1±12.8	42.0±5.1[a]	30.3±16.6[c]	0.014
Apex-1	30.0±5.6	45.5±6.8[a]	37.2±11.6[b]	<0.001	29.5±11.1	47.3±10.8[a]	32.5±16.8[c]	0.003
Apex	32.0±10.8	45.1±7.1[a]	38.6±14.7	0.014	32.5±12.0	44.5±7.0[b]	43.6±18.8[b]	0.029
Apex+1	34.3±10.5	46.5±9.4[b]	38.3±16.7	0.045	33.1±13.0	50.8±13.7[a]	44.5±14.0[b]	0.004
Apex+2	32.8±16.5	45.8±22.4	47.8±18.8[b]	0.071	40.6±12.6	47.1±16.0	52.6±13.4[b]	0.083
Total	30.8±8.1	45.1±7.7[a]	38.7±12.5[b]	0.001	32.6±10.9	46.3±7.3[a]	40.7±11.8[b]	0.004

Data are expressed as mean ± standard deviation. [a], P<0.01 when compared with Type A; [b], P<0.05 when compared with Type A; [c], P<0.01 when compared with Type B. PSM, paraspinal muscle.

between CBD and the total CSA of PSM in concavity (R=0.491, P=0.001) and convexity (R=−0.354, P=0.025). However, there no significant correlation between Cobb angle, SVA, TK and LL with the CSA at apex vertebra translation in concave and convex side (*Table 6*).

Discussion

Although coronal imbalance in patients with DS is quite common, the etiology for this occurrence remains unclear. Previous studies have indicated that bony structural changes may play a key role toward this deterioration (11,19,24).

Table 5 Pearson correlation analysis of Cobb angle and coronal balance distance on concave or convex cross-sectional area at the upper or lower intervertebral level of the apical vertebra

Variables	Cobb angle	Concavity						Convexity					
		Apex-2	Apex-1	Apex	Apex+1	Apex+2	Total	Apex-2	Apex-1	Apex	Apex+1	Apex+2	Total
Cobb angle (°)													
R	1.000	–0.288	–0.160	–0.431	–0.266	0.006	–0.287	–0.531	–0.433	–0.440	–0.330	–0.048	–0.415
P value	–	0.071	0.324	0.006	0.097	0.971	0.073	<0.001	0.005	0.004	0.038	0.769	0.008
CBD (cm)													
R	–0.006	0.148	0.215	0.183	–0.112	–0.021	0.085	–0.015	–0.035	–0.074	–0.121	–0.128	–0.089
P value	0.969	0.361	0.184	0.257	0.490	0.900	0.603	0.928	0.829	0.651	0.456	0.431	0.586
SVA (cm)													
R	–0.269	0.220	0.079	0.128	–0.007	–0.068	0.076	0.046	–0.026	–0.058	–0.056	–0.097	–0.048
P value	0.093	0.173	0.629	0.429	0.965	0.679	0.641	0.778	0.874	0.721	0.731	0.552	0.769
TK (°)													
R	0.073	0.160	0.269	0.225	0.218	0.130	0.252	0.172	0.358	0.365	0.306	0.118	0.319
P value	0.653	0.323	0.093	0.162	0.177	0.423	0.117	0.290	0.023	0.020	0.055	0.469	0.045
LL (°)													
R	0.151	–0.249	0.469	0.426	0.305	0.321	0.468	0.372	0.464	0.417	0.506	0.350	0.495
P value	0.352	0.121	0.002	0.006	0.055	0.043	0.002	0.018	0.003	0.007	0.001	0.027	0.001

CBD, coronal balance distance; SVA, sagittal vertical axis; TK, thoracic kyphosis; LL, lumbar lordosis; R, Pearson Correlation Coefficient.

Table 6 Pearson correlation analysis of Cobb angle and coronal balance distance on concave or convex fat infiltration at the upper or lower intervertebral level of the apical vertebra

Variables	Cobb angle	Concavity						Convexity					
		Apex-2	Apex-1	Apex	Apex+1	Apex+2	Total	Apex-2	Apex-1	Apex	Apex+1	Apex+2	Total
Cobb angle (°)													
R	1.000	0.046	0.007	–0.050	–0.069	–0.227	–0.097	0.000	–0.036	0.116	–0.011	–0.070	–0.001
P value	–	0.778	0.966	0.758	0.674	0.160	0.550	1.000	0.825	0.475	0.947	0.670	0.997
CBD (cm)													
R	–0.006	0.552	0.554	0.349	0.328	0.331	0.491	0.271	0.322	0.277	0.365	0.207	0.354
P value	0.969	<0.001	<0.001	0.027	0.039	0.037	0.001	0.090	0.042	0.084	0.021	0.200	0.025
SVA (cm)													
R	–0.269	0.444	0.426	0.227	0.292	0.209	0.365	0.318	0.305	0.168	0.229	0.115	0.277
P value	0.093	0.004	0.006	0.160	0.067	0.195	0.021	0.045	0.056	0.300	0.156	0.480	0.083
TK (°)													
R	0.073	–0.058	–0.222	–0.155	0.028	0.052	–0.062	0.109	0.117	0.035	0.004	0.013	0.067
P value	0.653	0.716	0.168	0.338	0.862	0.749	0.702	0.502	0.473	0.831	0.980	0.936	0.682
LL (°)													
R	0.151	0.056	–0.045	–0.006	–0.089	–0.009	–0.022	–0.039	–0.016	0.221	–0.108	0.004	0.013
P value	0.352	0.731	0.781	0.969	0.584	0.954	0.891	0.811	0.921	0.170	0.505	0.980	0.938

CBD, coronal balance distance; SVA, sagittal vertical axis; TK, thoracic kyphosis; LL, lumbar lordosis; R, Pearson correlation coefficient.

Owing to the interrelationship of muscle and bones, it has been suggested that PSM degeneration might play a role curve progression in DS patients with coronal imbalance (11,25). Based on this current study, this is the first to report that DS patients without coronal imbalance (Type A) would have lower FI% than those with coronal imbalance (Type B and Type C) in both concavity and convexity of the curve. Moreover, we showed a positive correlation between coronal imbalance distances and PSM degeneration in patients with DS.

In recent years, increasing attention was given toward the role of paraspinal muscle in pathogenesis of spinal disorders. Multiple studies have showed correlation between PSM degeneration with back pain, radiculopathy, and spinal deformity (19,21,26-28). Similarly, Lee *et al.* reported extensive degeneration of back muscle could be a causative factor in the pathogenesis of flat back syndrome (23). Correlation between PSM degeneration and spinopelvic parameters were comprehensively described by Xia *et al.* (29). In a study investigating the role of paraspinal muscle in AIS, Yeung *et al.* (10) describes asymmetrical fat composition and linear correlation between fat infiltration and curve magnitude. However, the contribution of paraspinal muscle degeneration is minor compared to that of DS. Yagi *et al.* (25) and Shafaq *et al.* (2) described more severe morphological and histological change in DS, which indicate muscle degeneration playing a more important role in the pathogenesis of DS. However, as most of those studies mainly focused on the contribution of PSM to sagittal parameters, it is often neglected toward its role on coronal imbalance.

The well accepted classification of adult spinal deformity-SRS-Schwab classification includes four main coronal curve types which mainly focused on sagittal malalignment while coronal imbalance was little involved (30). Coronal imbalance demonstrates various forms in DS. Nanjing classification concluded preoperative coronal imbalance in to three subtypes and emphasized its impact on postoperative outcomes. In this study, we hypothesized PSM degeneration may differ in three subtypes of coronal imbalance. The findings from our study will potentially help to provide new prospective, and to partially contribute, in the understanding on the pathogenesis of coronal imbalance.

In patients with degenerative lumbar kyphosis (DLK), Lee *et al.* (23) and Hyun *et al.* (31) found smaller CSA compared to healthy volunteers. Yagi *et al.* (25) found asymmetrical size of PSM, in which PSM in convex side

demonstrated larger CSA compared to concave side. Manion *et al.* (32) and Shafaq *et al.* (2) reported smaller fiber size and decreased nuclei in concave side compared to convex side of paraspinal muscle through histological study in DS patients, which also indicates more severe muscle degeneration in concave side. While cross-sectional area represents the paraspinal muscle volume, fat infiltration represents declining muscle structure and quality (33). High content of fat infiltration results in direct dysfunction of skeletal muscle (34,35). Tang *et al.* (36) found fat filtration was correlated with health related quality of life scores of DS patients while no significant correlation was found in terms of CSA. Though, smaller CSA also could represent PSM degeneration, however, we did not find any significant difference in terms of CSA of PSM between DS patients with and without coronal imbalance. This may indicate muscle volume is not sensitive to coronal imbalance. This further supported by our finding on the correlation between CSA and Cobb angle and CBD and FI%, respectively. Such that, the change of functional muscle mass to fat deposits during muscle degeneration may also help to explain our current observations.

Fat infiltration was reported to decrease the contractile composition of muscle mass which in turn leads to decline of production of musculature power (37). Grawford *et al.* (38) reported gradually increasing FI in lumbar paraspinal muscle from cranial to caudal side which was consistent with the result of our study. It showed higher FI% was significantly observed in patients with type B patients and type C when compared to type A. Moreover, FI% was found to be positively correlated with CBD at each level regardless of concave or convex side in present study. Taken together, we believe that high percentage of fat infiltration in PSM in type B, especially at upper levels, leads lower muscle strength in upper levels which may lead lower compensability to maintain spinal balance in upper segments of spine. Likewise, sever fat infiltration in lower levels of lumbar spine in type C patients may lead poor muscle strength at the base of spine and maybe readily decompensate to convex side. Several studies reported lower preoperative thoracolumbar muscle quality in patients with proximal junctional kyphosis (PJK) and even muscle degeneration as a risk factor for occurrence of PJK (39-41). Furthermore, several studies reported that poor muscle quality is correlated with distal screw loosening in patients with DS after corrective surgery (42-44).

There are several limitations in this study. Firstly, this is a retrospective study with relatively small sample size. High

standard for case-match analysis as well as strict criteria for collecting homogenous MRI sequence have limited the sample size. Secondly, although different state of PSM degeneration was found among three types of DS, it is still difficult to ascertain the casual relationship between PSM degeneration and scoliosis as retrospective nature of this study. Thus, long-term prospective studies are needed. In addition, the CSAs and FI% were measured at 2D plane which cannot precisely show the volume of muscle and fat, and 3D reconstruction of soft tissue and bone would provide a way to minimize the bias from manual measurement and positional change (24).

Conclusions

In conclusion, DS patients with coronal imbalance demonstrated a worse PSM degeneration, especially higher fat infiltration, when compared with those without coronal imbalance. In particularly, the increase of CBD significantly correlated with FI% at both concavity and convexity of the apical curve. This implies that PSM degeneration may contribute to the coronal imbalance in patients with DS. However, as cause-result relationship between scoliosis and PSM still difficult to ascertain, a longitudinal investigation is necessary to elucidate those findings.

Acknowledgments

Footnote

Reporting Checklist: The authors have completed the STROBE reporting checklist. Available at https://qims.amegroups.com/article/view/10.21037/qims-22-222/rc

Conflicts of Interest: All authors have completed the ICMJE uniform disclosure form (available at https://qims.amegroups.com/article/view/10.21037/qims-22-222/coif).

Ethical Statement: The authors are accountable for all aspects of the work in ensuring that questions related to the accuracy or integrity of any part of the work are appropriately investigated and resolved. The study was conducted in accordance with the Declaration of Helsinki (as revised in 2013). The study was approved by institutional review board (No. 2021-LCYJ-DBZ-05). All volunteers were fully informed about the methods, purposes, and risks involved in the study protocol and signed the informed consent.

Open Access Statement: This is an Open Access article distributed in accordance with the Creative Commons Attribution-NonCommercial-NoDerivs 4.0 International License (CC BY-NC-ND 4.0), which permits the non-commercial replication and distribution of the article with the strict proviso that no changes or edits are made and the original work is properly cited (including links to both the formal publication through the relevant DOI and the license). See: https://creativecommons.org/licenses/by-nc-nd/4.0/.

References

1. York PJ, Kim HJ. Degenerative Scoliosis. Curr Rev Musculoskelet Med 2017;10:547-58.
2. Shafaq N, Suzuki A, Matsumura A, Terai H, Toyoda H, Yasuda H, Ibrahim M, Nakamura H. Asymmetric degeneration of paravertebral muscles in patients with degenerative lumbar scoliosis. Spine (Phila Pa 1976) 2012;37:1398-406.
3. Koerner JD, Reitman CA, Arnold PM, Rihn J. Degenerative Lumbar Scoliosis. JBJS Rev 2015;3:e1.
4. Diebo BG, Shah NV, Boachie-Adjei O, Zhu F, Rothenfluh DA, Paulino CB, Schwab FJ, Lafage V. Adult spinal deformity. Lancet 2019;394:160-72.
5. Deng X, Zhu Y, Wang S, Zhang Y, Han H, Zheng D, Ding Z, Wong KK. CT and MRI Determination of Intermuscular Space within Lumbar Paraspinal Muscles at Different Intervertebral Disc Levels. PLoS One 2015;10:e0140315.

6. Peng X, Li X, Xu Z, Wang L, Cai W, Yang S, Liao W, Cheng X. Age-related fatty infiltration of lumbar paraspinal muscles: a normative reference database study in 516 Chinese females. Quant Imaging Med Surg 2020;10:1590-601.

7. Jun HS, Kim JH, Ahn JH, Chang IB, Song JH, Kim TH, Park MS, Chan Kim Y, Kim SW, Oh JK, Yoon DH. The Effect of Lumbar Spinal Muscle on Spinal Sagittal Alignment: Evaluating Muscle Quantity and Quality. Neurosurgery 2016;79:847-55.

8. Goubert D, Oosterwijck JV, Meeus M, Danneels L. Structural Changes of Lumbar Muscles in Non-specific Low Back Pain: A Systematic Review. Pain Physician 2016;19:E985-E1000.

9. Hiyama A, Katoh H, Sakai D, Tanaka M, Sato M, Watanabe M. The correlation analysis between sagittal alignment and cross-sectional area of paraspinal muscle in patients with lumbar spinal stenosis and degenerative spondylolisthesis. BMC Musculoskelet Disord 2019;20:352.

10. Yeung KH, Man GCW, Shi L, Hui SCN, Chiyanika C, Lam TP, Ng BKW, Cheng JCY, Chu WCW. Magnetic Resonance Imaging-Based Morphological Change of Paraspinal Muscles in Girls With Adolescent Idiopathic Scoliosis. Spine (Phila Pa 1976) 2019;44:1356-63.

11. Sun XY, Kong C, Zhang TT, Lu SB, Wang W, Sun SY, Guo MC, Ding JZ. Correlation between multifidus muscle atrophy, spinopelvic parameters, and severity of deformity in patients with adult degenerative scoliosis: the parallelogram effect of LMA on the diagonal through the apical vertebra. J Orthop Surg Res 2019;14:276.

12. Xu L, Sun X, Huang S, Zhu Z, Qiao J, Zhu F, Mao S, Ding Y, Qiu Y. Degenerative lumbar scoliosis in Chinese Han population: prevalence and relationship to age, gender, bone mineral density, and body mass index. Eur Spine J 2013;22:1326-31.

13. Maier SP, Smith JS, Schwab FJ, Obeid I, Mundis GM, Klineberg E, Hostin R, Hart RA, Burton D, Boachie-Adjei O, Gupta M, Ames C, Protopsaltis TS, Lafage V; International Spine Study Group. Revision Surgery After 3-Column Osteotomy in 335 Patients With Adult Spinal Deformity: Intercenter Variability and Risk Factors. Spine (Phila Pa 1976) 2014;39:881-5.

14. Glassman SD, Berven S, Bridwell K, Horton W, Dimar JR. Correlation of radiographic parameters and clinical symptoms in adult scoliosis. Spine (Phila Pa 1976) 2005;30:682-8.

15. Bao H, Yan P, Qiu Y, Liu Z, Zhu F. Coronal imbalance in degenerative lumbar scoliosis: Prevalence and influence on surgical decision-making for spinal osteotomy. Bone Joint J 2016;98-B:1227-33.

16. Cheng GHM, Yap WMQ, Kaliya-Perumal AK, Oh JY. Correction of degenerative lumbar coronal deformity using asymmetrical interbody cages: Surgical technique and case report. J Craniovertebr Junction Spine 2021;12:432-6.

17. Mundis GM Jr, Walker CT, Smith JS, Buell TJ, Lafage R, Shaffrey CI, Eastlack RK, Okonkwo DO, Bess S, Lafage V, Uribe JS, Lenke LG, Ames CP; International Spine Study Group (ISSG). Kickstand rods and correction of coronal malalignment in patients with adult spinal deformity. Eur Spine J 2022;31:1197-205.

18. Theologis AA, Lertudomphonwanit T, Lenke LG, Bridwell KH, Gupta MC. The role of the fractional lumbosacral curve in persistent coronal malalignment following adult thoracolumbar deformity surgery: a radiographic analysis. Spine Deform 2021;9:721-31.

19. Xie D, Zhang J, Ding W, Yang S, Yang D, Ma L, Zhang J. Abnormal change of paravertebral muscle in adult degenerative scoliosis and its association with bony structural parameters. Eur Spine J 2019;28:1626-37.

20. Johannesdottir F, Allaire B, Anderson DE, Samelson EJ, Kiel DP, Bouxsein ML. Population-based study of age- and sex-related differences in muscle density and size in thoracic and lumbar spine: the Framingham study. Osteoporos Int 2018;29:1569-80.

21. Smith JA, Stabbert H, Bagwell JJ, Teng HL, Wade V, Lee SP. Do people with low back pain walk differently? A systematic review and meta-analysis. J Sport Health Sci 2022;11:450-65.

22. Kuklo TR, Potter BK, Polly DW Jr, O'Brien MF, Schroeder TM, Lenke LG. Reliability analysis for manual adolescent idiopathic scoliosis measurements. Spine (Phila Pa 1976) 2005;30:444-54.

23. Lee JC, Cha JG, Kim Y, Kim YI, Shin BJ. Quantitative analysis of back muscle degeneration in the patients with the degenerative lumbar flat back using a digital image analysis: comparison with the normal controls. Spine (Phila Pa 1976) 2008;33:318-25.

24. Ferrero E, Skalli W, Lafage V, Maillot C, Carlier R, Feydy A, Felter A, Khalifé M, Guigui P. Relationships between radiographic parameters and spinopelvic muscles in adult spinal deformity patients. Eur Spine J 2020;29:1328-39.

25. Yagi M, Hosogane N, Watanabe K, Asazuma T, Matsumoto M; Keio Spine Research Group. The paravertebral muscle and psoas for the maintenance of global spinal alignment in patient with degenerative

---

lumbar scoliosis. Spine J 2016;16:451-8.

26. Barker KL, Shamley DR, Jackson D. Changes in the cross-sectional area of multifidus and psoas in patients with unilateral back pain: the relationship to pain and disability. Spine (Phila Pa 1976) 2004;29:E515-9.

27. Yoshihara K, Shirai Y, Nakayama Y, Uesaka S. Histochemical changes in the multifidus muscle in patients with lumbar intervertebral disc herniation. Spine (Phila Pa 1976) 2001;26:622-6.

28. Wu Z, Ye X, Ye Z, Hong K, Chen Z, Wang Y, Li C, Li J, Huang J, Zhu Y, Lu Y, Liu W, Xu X. Asymmetric Biomechanical Properties of the Paravertebral Muscle in Elderly Patients With Unilateral Chronic Low Back Pain: A Preliminary Study. Front Bioeng Biotechnol 2022;10:814099.

29. Xia W, Fu H, Zhu Z, Liu C, Wang K, Xu S, Liu H. Association between back muscle degeneration and spinal-pelvic parameters in patients with degenerative spinal kyphosis. BMC Musculoskelet Disord 2019;20:454.

30. Schwab F, Ungar B, Blondel B, Buchowski J, Coe J, Deinlein D, DeWald C, Mehdian H, Shaffrey C, Tribus C, Lafage V. Scoliosis Research Society-Schwab adult spinal deformity classification: a validation study. Spine (Phila Pa 1976) 2012;37:1077-82.

31. Hyun SJ, Bae CW, Lee SH, Rhim SC. Fatty Degeneration of the Paraspinal Muscle in Patients With Degenerative Lumbar Kyphosis: A New Evaluation Method of Quantitative Digital Analysis Using MRI and CT Scan. Clin Spine Surg 2016;29:441-7.

32. Mannion AF, Meier M, Grob D, Müntener M. Paraspinal muscle fibre type alterations associated with scoliosis: an old problem revisited with new evidence. Eur Spine J 1998;7:289-93.

33. Crawford RJ, Elliott JM, Volken T. Change in fatty infiltration of lumbar multifidus, erector spinae, and psoas muscles in asymptomatic adults of Asian or Caucasian ethnicities. Eur Spine J 2017;26:3059-67.

34. Elliott JM, Kerry R, Flynn T, Parrish TB. Content not quantity is a better measure of muscle degeneration in whiplash. Man Ther 2013;18:578-82.

35. Greve T, Burian E, Zoffl A, Feuerriegel G, Schlaeger S, Dieckmeyer M, Sollmann N, Klupp E, Weidlich D, Inhuber S, Löffler M, Montagnese F, Deschauer M, Schoser B, Bublitz S, Zimmer C, Karampinos DC, Kirschke JS, Baum T. Regional variation of thigh muscle fat infiltration in patients with neuromuscular diseases compared to healthy controls. Quant Imaging Med Surg 2021;11:2610-21.

36. Tang Y, Yang S, Chen C, Luo K, Chen Y, Wang D, Tan J, Dai Q, Zhang C, Wu W, Xu J, Luo F. Assessment of the association between paraspinal muscle degeneration and quality of life in patients with degenerative lumbar scoliosis. Exp Ther Med 2020;20:505-11.

37. Fidler MW, Jowett RL. Muscle imbalance in the aetiology of scoliosis. J Bone Joint Surg Br 1976;58:200-1.

38. Crawford RJ, Volken T, Ni Mhuiris Á, Bow CC, Elliott JM, Hoggarth MA, Samartzis D. Geography of Lumbar Paravertebral Muscle Fatty Infiltration: The Influence of Demographics, Low Back Pain, and Disability. Spine (Phila Pa 1976) 2019;44:1294-302.

39. Hyun SJ, Kim YJ, Rhim SC. Patients with proximal junctional kyphosis after stopping at thoracolumbar junction have lower muscularity, fatty degeneration at the thoracolumbar area. Spine J 2016;16:1095-101.

40. Pennington Z, Cottrill E, Ahmed AK, Passias P, Protopsaltis T, Neuman B, Kebaish KM, Ehresman J, Westbroek EM, Goodwin ML, Sciubba DM. Paraspinal muscle size as an independent risk factor for proximal junctional kyphosis in patients undergoing thoracolumbar fusion. J Neurosurg Spine 2019;31:380-8.

41. Yuan L, Zeng Y, Chen Z, Li W, Zhang X, Mai S. Degenerative lumbar scoliosis patients with proximal junctional kyphosis have lower muscularity, fatty degeneration at the lumbar area. Eur Spine J 2021;30:1133-43.

42. Kim JB, Park SW, Lee YS, Nam TK, Park YS, Kim YB. The Effects of Spinopelvic Parameters and Paraspinal Muscle Degeneration on S1 Screw Loosening. J Korean Neurosurg Soc 2015;58:357-62.

43. Leng J, Han G, Zeng Y, Chen Z, Li W. The Effect of Paraspinal Muscle Degeneration on Distal Pedicle Screw Loosening Following Corrective Surgery for Degenerative Lumbar Scoliosis. Spine (Phila Pa 1976) 2020;45:590-8.

44. Wang W, Li W, Chen Z. Risk factors for screw loosening in patients with adult degenerative scoliosis: the importance of paraspinal muscle degeneration. J Orthop Surg Res 2021;16:448.